Review of sulfur dioxide to sulfate aerosol chemistry at Kīlauea Volcano, Hawai‘i

by

Andre Pattantyus, Steven Businger, and Steven Howell

University of Hawai‘i at Mānoa,

Honolulu, HI, USA

Key points:

1. OH dominates oxidation of SO_2 at Kīlauea in the gas phase and H_2O_2 in the aqueous phase.
2. High SO_2 emissions and volcanic bromine limit gas phase oxidation and prolong SO_2 lifetime.
3. Secondary aqueous phase reactions may become important for SO_2 concentrations $\geq$ 10 ppm.

© 2018. This manuscript version is made available under the Elsevier user license
http://www.elsevier.com/open-access/userlicense/1.0/

Abstract

Sulfur dioxide emissions from the Kīlauea Volcano on the island of Hawai‘i and the subsequent formation of sulfate aerosols have caused a public health hazard across the state of Hawai‘i since the volcano began erupting continuously in 1983. The University of Hawai‘i at Mānoa began to forecast the trajectory and dispersion of emissions in 2010 to help mitigate the hazards to public health. In this paper a comprehsive review of potential conversion reactions is presented with the goal of more accurately representing the sulfur dioxide chemistry in the dispersion model.

Atmopheric sulfur dioxide chemistry and major process responsible for sulfate formation are well documented in urban and industrial settings. The atmosphere in the vicinity of Kīlauea Volcano on the island of Hawai‘i differs from that in previous investigations by virtue of being far removed from both urban and industrial settings in a remote, tropical marine atmosphere. Additionally, the combination of the high rate of sulfur dioxide emissions and trace gases and metals from Kīlauea Volcano creates a unique circumstance that requires a new look at potential conversion pathways to determine the dominant reactions.

The theoretical analysis suggests that the dominant reaction in clear air will be between sulfur dioxide and the hydroxyl radical (0.01 to 5% h^{-1}) and the dominant reaction in cloudy air involves hydrogen peroxide (3-50% s^{-1}). Morevover, given the high SO_2 emissions from the Halema‘uma‘u Crater vent, the oxidation of sulfur dioxide by these reactants is limited by their rate of production.

Keywords: sulfur chemistry, sulfate aerosols, volcanic emissions, vog

1. Introduction

Since 1983, Kīlauea volcano has been continuously erupting from the Pu‘u ‘Ō‘o vent, or East Rift vent, emitting large amounts of sulfur dioxide (SO_2). The rate of SO_2 emissions has ranged from less than 50 tons per day (t d^{-1}) to more than 10,000 t d^{-1} [Elias and Sutton, 2007]. In 2008, a second vent opened up in the Halema‘uma‘u Crater, or summit vent, with a typical emission rate of ~1000 to 3000 t d^{-1} estimated from ground-based remote sensing observations [Elias and Sutton, 2012]. This leads to annual SO_2 emissions between 0.3 and 1.1 million tons. In comparison, the 50 dirtiest power plants in the United States emit between 0.04 and 0.2 millions tons of SO_2 annually [Environmental Integrity Project, 2007].

Given the persistent northeast trade winds in tropical North Pacific, emissions from Kīlauea cause frequent episodes of poor air quality in the form of volcanic smog, or vog, over downwind and leeward communities on the island of Hawai‘i. Vog is composed of sulfur dioxide gas, the primary pollutant emitted by the volcano, and sulfate aerosols, a secondary pollutant that forms from the oxidation of sulfur dioxide. Between 2007 and 2010, it is estimated that Kīlauea volcano was responsible for 6% of global sulfate load [Elias and Sutton, 2012]. Due to their size, sulfate aerosols are considered a dominant component of fine particulate matter smaller than 2.5 micrometers ($PM_{2.5}$) and can impact human health and reduce visibility. Communities in close proximity to the volcano, such as the village of Volcano, are especially susceptible to episodes of poor air quality from SO_2 pollution, (Figure 1) some of which have reached levels high enough that evacuations were ordered.

While the lifetime of sulfur dioxide in the atmosphere is generally found to be on the order of 1-3 days [Rotstayn and Lohmann, 2002], the lifetime of sulfates can be much longer. The lifetime of SO_2 is limited by ubiquitous photochemical sinks whereas the lifetime of sulfate is limited by a relatively slow rate of dry deposition and the erratic nature of wet deposition. Due to longer residence times, sulfate impacts can become pervasive. Hand et al. [2012] showed that long range transport of sulfates from Asia impact air quality in the Pacific Northwest. It has also been demonstrated that Hawai‘i is affected by Asian aerosols from March to May that includes measurable sulfate [Shaw, 1980; Perry et al., 1999; Holben et al. 2001].

Given the variety of negative impacts from sulfate aerosols [Businger et al., 2015], it is important to determine the rate of sulfate formation from sulfur dioxide emitted naturally and by industry. There are a number of active volcanoes worldwide that degas sulfur dioxide (http://so2.gsfc.nasa.gov/), leading to sulfates that regularly impact the air quality of a number of communities including those in Iceland, Nicaragua, Italy, and the Caribbean. Coal-burning power plants and industrial smelters also produce large amounts of sulfur dioxide and sulfates. The rapid expansion of coal power plants in China and India has led to hazardous air quality impacting local communities, neighboring countries, and locations far downwind [e.g., Hand et al., 2012].

Many attempts have been made to measure sulfur dioxide loss rates from volcanic emissions, including some in the lower troposphere or planetary boundary layer [McGonigle et al., 2004; Rodriguez et al., 2005; Oppenheimer et al., 1998; Porter et al. 2002; Kroll et al., 2015]. Generally, little care is taken during these experiments to attribute SO_2 loss to a particular process because the goal is only to determine if SO_2 flux

92 measurements from correlation spectrometers are reliable proxies for source emissions of
93 ash free tropospheric plumes [McGonigle et al., 2004]. The loss rate of SO_2 is important
94 for evaluating the uncertainty of volcanic emissions. If a signifcant portion of SO_2 is lost
95 between emission and measurement then fluxes would not be representative of the real
96 emission rate. Loss rates (s^{-1}), k, are calculated using an exponential decay equation

$$\Phi = \Phi_0 e^{-kt} \quad (1)$$

97 where Φ and Φ_0 represent SO_2 fluxes estimated from transects with correlation
98 spectometers taken at various distances downwind separated by some time, t. An implicit
99 assumption in equation 1 is that loss rates are a first order process with respect to SO_2
100 concentrations. A brief summary of previous SO_2 loss rate estimates at volcanoes found
101 in the tropics are presented in table 1. McGonigle et al. [2004] found moderate loss rates
102 at Mayasa volcano, Nicaragua. A majority of this loss rate was later attributed to plume
103 dispersion caused by accelerated wind speeds between observation sites suggesting a
104 very slow loss rate via gaseous conversion [Nadau, 2006]. Comparatively, Rodriguez et
105 al. [2005] estimated loss rates at Soufrière Hills volcano, Monserrat, British Virgin
106 Islands that ranged from relatively slow conversion (5%) to nearly total depletion of SO_2
107 (95%) over the course of an hour. Oppenheimer et al. [1998] found rates an order of
108 magnitude greater than Rodriquez et al. [2005] at Soufrière Hill, but noted that the plume
109 was entrained into orographic clouds. There is a large difference in the conversion rates
110 that can be explained by the various oxidation pathways responsible for the conversion.
111 The implicit assumption is that most lost SO_2 is converted to sulfate aerosols.
112 Oppenheimer et al. [1998] caution that their observations of the rapid loss of volcanic

113 SO_2 in-cloud could lead to a global underestimation of volcanic SO_2 and subsequently
114 underestimate tropospheric sulfate and its impacts on climate.
115 Estimates of sulfate production from Kīlauea calculated using ground-based
116 remote sensing methods imply a rate between 7 - 18% an hour [Porter et al., 2002]. This
117 assumes no primary sulfate being emitted, which may be incorrect based on near-vent
118 measurements by Mather et al. [2012] who found approximately 1% sulfate relative to
119 SO_2 emissions during the early eruptive period of Halema‘uma‘u in 2008. This
120 observation suggests a co-emitted catalyst (e.g., Fe^{2+}) may cause significant sulfate
121 formation as SO_2 exits the vent, inflating conversion rates estimated further downwind.
122 Such reactions have been implied previously [Eatough et al., 1984].
123 Kroll et al. [2015] measured ground-level sulfur dioxide and sulfate aerosols
124 downwind of Kīlauea simultaneously. They found SO_2 oxidation by OH to be the likely
125 conversion pathway but the conversion rate was much slower than previous estimates
126 likely due to OH depletion from high SO_2 emissions.
127 Conversion rates and processes observed in other locales may not apply at
128 Kīlauea given its unique features. Unlike many other volcanoes in the tropics that emit
129 into the free troposphere, Kīlauea emits SO_2 into the marine boundary layer. The
130 isolation of Kīlauea from major pollution sources within the tropical marine boundary
131 layer results in a unique set of environmental conditions not previously documented.
132 Ozone (O_3) and nitrogen oxides (NO_x) are found at much lower concentrations in the
133 remote marine boundary layer than the oft-studied power plant plumes. The Hawai‘i
134 Department of Health [2013] estimated all anthropogenic sources of SO_2 on Hawai‘i
135 island amount to less than 0.5% of the annual SO_2 emissions from Kīlauea. The high SO_2

136 emission rate at Kīlauea is at least an order of magnitude greater than those observed at
137 other volcanoes that SO_2 loss rates have been estimated [McGonigle et al., 2004; Nadau,
138 2006; Oppenheimer et al., 1998]. Large, periodic volcanic eruptions can be orders of
139 magnitude larger, such as the 1984 eruption of Mauna Loa [Sharma et al., 2004] or 2014-
140 2015 eruption of the Bárðarbunga volcanic system in Iceland [Gauthier et al., 2016].
141 Sharma et al. [2004] estimated the total SO_2 load from Mauna Loa to be 1.0 ± 0.2 Mt in
142 less than one month. Gauthier et al. [2016] estimated the SO_2 flux was 4 to 10 times the
143 current flux at Kīlauea but lasted for less than a year. The persistent abundance of SO_2 at
144 Kīlauea could deplete typical reactants rapidly, limiting conversion rates and increasing
145 the likelihood that additional trace gases and/or metals either emitted or in the ambient
146 environment could become important reactants themselves.
147 Chemical kinetic theory and observations have shown differences in the
148 efficiency between cloud-free, gas phase oxidation of sulfur dioxide and aqueous, in-
149 cloud oxidation. There are a number of variables that are thought to influence these
150 processes. Among them are solar insolation, atmospheric mixing, temperature, relative
151 humidity (RH), pH of cloud droplets, and species' concentrations [Eatough et al., 1994].
152 In this study, two dominant reaction pathways have been identified for the
153 oxidation of sulfur dioxide in Hawai‘i. The gas phase pathway is via reaction with the
154 hydroxyl radical, OH. The aqueous phase pathway is via reaction with hydrogen
155 peroxide, H_2O_2. Given chemical kinetic theory, what range of conversion rates can one
156 expect in the presence of SO_2 emissions from Kīlauea volcano? This will be addressed
157 through a detailed examination of the reaction kinetics of SO_2 with the hydroxyl radical
158 and hydrogen peroxide, including determinations of important variables that influence

159 SO_2 to sulfate conversion. Theoretical conversion rates are then estimated with locally
160 observed quantities and compared with past research. Lastly, the uncertainty of
161 theoretical conversion rates is discussed to highlight the difficulty in estimating the
162 quantity and provides a baseline for conversion rate estimates from observations.

163 It is the goal of this research to quantify the conversion rate of sulfur dioxide to
164 sulfate aerosol downwind of Kīlauea volcano on the island of Hawai‘i. Several
165 measurement campaigns found sulfur dioxide loss rates, but the distinction between the
166 gas phase and aqueous phase conversion has not been made clear in many instances
167 resulting in large uncertainty in loss rates. Observations during these campaigns suggest
168 that sulfur dioxide emissions interacting with clouds or fog produce substantially more
169 sulfate aerosols than through processes in clear air. It is the clear-air gas conversion that
170 will impact ground-level concentrations of SO_2 and sulfate aerosols regularly and is of
171 great interest here. Furthermore, only Porter et al. [2002] quantified sulfate production
172 rates from volcanic emissions by measuring sulfur dioxide and aerosols simultaneously.

173 Kīlauea is situated close (350 km) to large population centers (greater Honolulu –
174 population ~1 million) than most effusive volcanoes making the persistent eruptions an
175 ongoing public health issue. The application of this work is to improve forecasts for
176 ground level SO_2 and SO_4 by of the University of Hawaii Vog Model [Businger et al.,
177 2015]. Preliminary model evaluation revealed poor forecast skill in both species at
178 intermediate distances downwind. The goal is to improve forecast skill by replacing a
179 constant SO_2 to SO_4 conversion rate, representative of bulk conversion at daily to
180 monthly timescales, with first order conversion rates representative of gas and aqueous
181 phase oxidation. A conversion scheme that follows the first-order conversion pathways

182 is anticipated to improve forecast skill at timescales on the order of an hour and spatial
183 scales on the order of kilometers while not resulting in a significant increase in
184 computation time or resources that may delay forecast delivery to the public.
185 This paper will be organized into three sections. Sulfur chemistry in the gas phase
186 is presented in section two. Aqueous phase sulfur chemistry is discussed in section three.
187 Section four provides a summary of the dominant sulfur dioxide reaction pathways
188 around Kīlauea Volcano.
189
190 **2. Gas Phase**
191 Past research has determined that only the hydroxyl radical, OH, is important for
192 the oxidation of sulfur dioxide to sulfate aerosol in the gas phase during daytime
193 [Rattigan et al., 2000; Eatough et al., 1994 and references therein]. The latest data from
194 the Jet Propulsion Laboratory (JPL) shows that most reactions can be discounted based
195 on their reaction rate constants (Table 2) [Buckholder et al., 2015]. Oxidation via the
196 Criegee intermediates can also be discounted because the requisite reactants to make
197 Criegee radicals are absent.
198 The hydroxyl radical is formed through photolytic reactions and therefore has
199 diurnal and seasonal cycles. OH is considered the most important oxidizing agent in the
200 atmosphere because it is extremely reactive and able to oxidize most chemicals found in
201 the atmosphere [ESPERE Climate Encyclopedia, 2006]. Despite being highly reactive,
202 OH concentrations remain relatively constant at timescales of days to weeks (~ 1.0 part
203 per trillion or ppt), meaning production and loss rates are in quasi-steady state. Ozone
204 (O_3) is considered the main precursor for OH formation while in the remote marine

boundary layer OH is removed through reactions with carbon monoxide (CO) and methane (CH_4). At longer time scales, ozone concentrations follow an annual cycle, with near surface concentrations nearly doubling from austral winter to summer in Fiji [Takashima et al., 2007]. This implies an annual cycle in OH formation. Eatough et al. [1994] further suggest that OH formation is humidity dependent (via ozone), which will cause spatial and temporal variability on the scale of synoptic to mesoscale weather systems.

Once OH is formed the main reaction pathway with SO_2 is:

$$OH + SO_2 + (O_2, N_2) \Rightarrow HOSO_2 + (O_2, N_2) \quad (2)$$

$$HOSO_2 + O_2 \Rightarrow SO_3 + HO_2 \quad (3)$$

$$SO_3 + H_2O \Rightarrow H_2SO_4 \quad (4)$$

A significant fraction of $HOSO_2$ eventually becomes H_2SO_4. Reaction 2, between OH with SO_2, is known to be the rate-limiting step in the oxidation of sulfur dioxide to sulfate aerosol. The formation rate of sulfate aerosol, S, can be solved via

$$S = k_c[SO_2][OH] \quad (5)$$

where k_c is the conversion rate constant (cm^3 $molecules^{-1}$ s^{-1}), and $[SO_2]$ and [OH] are species concentrations (molecules cm^{-3}) [Raes et al., 1992; Simpson, 2010].

Many values have been obtained for k_c at different reference temperatures. The uncertainty of k_c, according to Atkinson et al. [1989], is of the order of a factor 2($\Delta\log(k) = \pm 0.3$). Based on this uncertainty, Raes et al. [1992] used a range of k_c values from 4.5 x 10^{-13} to 2.4 x 10^{-12} cm^3 $molecules^{-1}$ s^{-1} to determine model sensitivity. They found that model results match smog chamber results for a range of values from 7.8 x 10^{-13} to 1.0 x 10^{-12} cm^3 $molecules^{-1}$ s^{-1}. For comparison, the JPL recommended value for k = 1.6 x 10^{-}

^{12} cm^3 molecules^{-1} s^{-1} at a temperature of 300 K [Sander et al., 2011] falls within the range of estimates by Raes et al. [1992].

The reaction represented by equation (2) is thought to be a function of temperature and relative humidity (via OH production). Eatough et al. [1994] developed two equations to incorporate the moisture and temperature dependence into calculations for the first order rate coefficient, k_1. The moisture dependence is described by the dewpoint temperature (T_D) and reference values of k_1 and T_D at 25°C (Eq. 6). The temperature dependence was found through a linear regression fit of 109 k_1 values to 1/T (K) (Eq. 7). This fit was performed by normalizing all values to 50% RH. The conversion rate at any temperature, T, calculated from equation 7 can be converted to any RH using equation 6 [Eatough et al. 1994]. The resulting solution for k_1 is seen in figure 8.

$$\frac{\Delta \ln k_1}{\Delta T_D} = 0.0452°C^{-1} \tag{6}$$

$$\ln k_1 = (24.91 \pm 0.41) - (8290 \pm 390)/T \tag{7}$$

$$k_1 = e^{\left([(24.91 \pm 0.41) - (8290 \pm 390)/T] - \Delta T_D \times 0.0452°C^{-1}\right)} \tag{8}$$

The result of equation 8 is a unitless value. In order to use k_1 in equation 5 we must put it in correct units and also scale it appropriately. Without scaling the value is simply a first order bulk conversion rate that does not take into account diurnal variations in OH. Based on reported values of k_c and values reported by Eatough et al. [1994], k_1 from equation 8 is scaled by 1.0 x 10^{-12} cm^3 molecules^{-1} s^{-1}.

In order to solve equation 5, OH concentrations have to either be measured or modeled with a photochemical model. Although OH is not routinely observed, past field

243 campaigns have collected OH data. The most geographically specific data to Hawai‘i is
244 from INTEX-B [Singh et al., 2008], which was collected between 05 and 07 UTC 1 May
245 2006. Although this was an overnight flight, it provides a lower bound on the OH diurnal
246 cycle. A mean OH concentration of approximately .01 ppt (~2.5 x 10^5 molecules cm^{-3}) is
247 found.

248 The diurnal cycle of OH is best illustrated in figure 2 with data from the INTEX-
249 B flights near Hawaii (region 4 in Singh et al., 2008). Flights were flown from April 17
250 to May 1 over the Pacific Ocean. Data collected between -180° W and -140° W and
251 18°N and 40°N are displayed in figure 2. Several legs were flown near the surface during
252 both day and night. Daytime concentrations peaked between 6 x 10^6 molecules cm^{-3} and
253 1 x 10^7 molecules cm^{-3} with nighttime concentrations approximately two orders of
254 magnitude lower.

255 Further studies have found similar diurnal cycles of OH in the mid-latitudes
256 during various seasons [Forberich et al., 1999; Hand et al., 1991]. Hand et al. [1991]
257 found a range of OH concentrations from a peak of 4 x 10^6 molecules cm^{-3} during the day
258 to a minimum that oscillated about 1 - 5 x 10^5 molecules cm^{-3} overnight. Forberich et al.
259 [1999] found a larger daytime range over several days from an early morning minimum
260 on the order of 10^5 molecules cm^{-3} to a maximum of 8-11 x 10^6 molecules cm^{-3}.

261 Hypothetical limits of sulfur dioxide oxidation by the hydroxyl radical can be
262 calculated with the use of values from figure 2 and equation (5). For this calculation
263 hourly average temperature and RH values from 20 July 2014 at Hawai‘i Volcanoes
264 National Park Observatory (HAVO-OB) were used to determine *k* (Table 3). This site is
265 chosen for its proximity to the Halema‘uma‘u Crater vent. Over the period of

266 measurement at HAVO-OB from initial deployment in 2011 to July 2014, the median
267 SO_2 concentration measured was approximately 2.46 x 10^{11} molecules cm^{-3} (10 ppb).
268 This value is used for both daytime and nighttime calculations. OH concentrations are
269 obtained from INTEX-B flights presented in figure 2 to represent the diurnal range of
270 concentrations with a daytime concentration of 1.0 x 10^7 molecules cm^{-3} and nocturnal
271 concentration of 2 x 10^5 molecules cm^{-3}. Previous measurement campaigns have also
272 found nocturnal OH concentrations in the range 2 x 10^5 to 10^6 molecules cm^{-3} [Brown
273 and Stutz, 2012]. Given that tradewinds are persistent near Halema‘uma‘u Crater, we
274 assume that a persistent supply of OH is advected into the region of the plume for
275 reaction with emitted SO_2. The subsequent k values calculated from equations (6) and
276 (7) were 4.04 x 10^{-13} cm^3 $molecules^{-1}$ s^{-1} and 5.58 x 10^{-13} cm^3 $molecules^{-1}$ s^{-1} for night and
277 day, respectively. The difference in k values is approximately 30%, given the relatively
278 small ΔT (4.8°C) and ΔRH (21%). If one assumes 100% conversion, this results in SO_2 to
279 sulfate conversion rates of 1.98 x 10^4 cm^3 $molecules^{-1}$ s^{-1} and 1.37 x 10^6 cm^3 $molecules^{-1}$
280 s^{-1} for night and day, respectively. That works out to 7.13 x 10^7 molecules cm^{-3} h^{-1} and
281 4.9 x 10^9 molecules cm^{-3} h^{-1} for night and day, respectively. By percentage of SO_2
282 concentration for each time period that works out to a rate of .03% h^{-1} and 2% h^{-1} for
283 nighttime and daytime.

284 These rates of sulfate formation are similar to those of Kroll et al. [2015] and
285 lower than those found by Porter et al. [2002] but are within the range of values for SO_2
286 loss found elsewhere [McGonigle et al., 2004; Rodriguez et al., 2005]. The uncertainty
287 in *k,* resulting from the temperature dependence represented in equation (7), results in a
288 range from 2.29 x 10^{-13} to 1.42 x 10^{-12} molecules cm^{-3} s^{-1} during the day and 1.64 x 10^{-13}

289 to 1.06 x 10^{-12} molecules cm^{-3} s^{-1} at night. The corresponding conversion rate range is 0.8
290 - 5% h^{-1} during the day and 0.01 - 0.07% h^{-1} at night. A more thorough treatment of the
291 uncertainty in the conversion rate would take into account the variability in OH
292 concentrations as well, however even when considering uncertainty in OH a majority of
293 theoretical conversion rates will fall within the range of values found above which were
294 calculated with the extreme values of OH concentration measured during INTEX-B.
295 It is important to note that theoretical conversion rate coefficients are meant to
296 represent standard atmospheric conditions. A typical atmospheric concentration of SO_2 is
297 in the range of 1-100 ppt (2.46 x 10^7 molecules cm^{-3} to 2.46 x 10^9 molecules cm^{-3}), much
298 lower than the concentration used above (10 ppb). SO_2 concentrations can easily exceed
299 100 ppm (2.46 x 10^{15} molecules cm^{-3}) above Halema‘uma‘u Crater vent (Andrew Sutton
300 2015, personal communication). Given such high concentrations of SO_2, eight to nine
301 orders of magnitude greater than OH, the reaction rate would be limited by OH
302 concentrations and how rapidly OH can be produced.
303 Because the concentration of OH is considered steady state, the
304 environmental formation rate can be approximated by the loss rate via carbon
305 monoxide (CO) and methane (CH_4). CO and CH_4 would be the leading reactants with
306 OH in the marine boundary layer given the absence of volatile organic compound
307 (VOC) sources upwind. Concentration data for these gases were available from the
308 INTEX-B data set. The loss/production rate was estimated via

$$\frac{d\mathrm{OH}}{dt} = k_{CO}[\mathrm{OH}][\mathrm{CO}] + k_{CH4}[\mathrm{OH}][\mathrm{CH_4}] \quad (9)$$

309 where [CO] is the atmospheric concentration of carbon monoxide, [CH_4] is the
310 concentration of methane, k_{CO} = 3.45 x 10^{-13} cm^3 $molecules^{-1}$ s^{-1} [Baulch et al., 1980],

311 and k_{CH4} = 6.3 x 10^{-15} cm^3 $molecules^{-1}$ s^{-1} [Sander et al., 2011]. The loss/production
312 rate of OH was approximately 2 x 10^{-8} molecules cm^{-3} s^{-1} and was dominated by
313 reactions with CO. This represents a cap on OH reactions with SO_2, which would
314 have been reached as SO_2 concentrations approached 1 x 10^{14} (~10 ppm) during
315 maximum OH concentrations. This limit remained proportional to SO_2
316 concentrations throughout the diurnal cycle (Figure 3). For our purposes, we
317 assume that mixing between the plume and the environment over periods of tens of
318 minutes lead to near steady-state concentrations of OH even in the presence of SO_2
319 plumes.
320 The model sensitivity study of Jourdain et al. [2016] found the depletion of O_3
321 by halogen reactions led to decreases in OH, beyond those associated with reactions
322 with SO_2, resulted in ~30% longer SO_2 lifetimes. In their Ambrym simulations,
323 halogen ratios such as HBr/SO_2 and HCl/SO_2, were estimated to be an order of
324 magnitude more abundant than observations of halogens at Kilauea [Mather et al.,
325 2012], while Ambrym SO_2 emissions were 4-6x as great as Kīlauea meaning actual
326 HBr emission rates are two orders of magnitude lower at Kīlauea. Although some
327 depletion may be occurring within the Kīlauea plume due to halogen and SO_2
328 reactions, the magnitude is likely lower given the lower abundance of both SO_2 and
329 halogens.
330 Other studies have found a reduction in O_3 in SO_2 plumes, which also limits
331 the production of OH via halogen reactions [Vance et al., 2010; Oppenheimer et al.,
332 2010; Schuman et al., 2011; Kelly et al., 2013; Surl et al., 2015]. Surl et al. [2015]
333 find the typical range of HBr/SO_2 measured at various volcanoes to encompass the

334 values measured at Kīlauea. These studies suggest the limit of OH production in SO_2
335 plumes is as much as 30% lower than the OH production rate calculation.
336 In summary, theoretical gas phase conversion rates estimated for conversion of
337 SO_2 to sulfate aerosol display rates less than 10% h^{-1}. Daytime conversion rates are
338 estimated to be 2.9 ± 2.1 % h^{-1}, while nighttime conversion rates are estimated to be 0.04
339 ± 0.3 % h^{-1}. Very high concentrations of SO_2 have been observed near the vents and
340 could lead to this reaction being severely limited by availability of OH. Additionally, in-
341 plume OH limiting reactions via HBr could further reduce SO_2 conversion rates by as
342 much as 30%.
343 There is some uncertainty in the OH conversion rate that stems from the
344 temperature and moisture dependence of the reaction between OH and SO_2, which is
345 represented in the conversion rate coefficient, k. Sander et al. [2011] suggest the
346 uncertainty associated with the temperature dependence of the reaction is minimized near
347 room temperatures (25-27°C) - a temperature range typical of Hawai‘i’s climate.
348 Additional uncertainty will arise from OH concentrations, including reduction of OH
349 from in-plume halogen chemistry, and OH delivered to the plume through mixing
350 between the plume and environment.
351
352 **3. Aqueous Phase**
353 If the SO_2 plume encounters a cloud then SO_2 can be taken up in cloud water and
354 undergo oxidation via aqueous phase pathways. Though this discussion will be limited to
355 in-cloud oxidation it is possible that some loss of gas-phase SO_2 may occur due to mass
356 transfer to aerosols.

357 Faloona et al. [2009] and Faloona [2009] have argued that SO_2 mass transfer to
358 coarse mode sea salt aerosols (SSA) in non-negligible. This process is highly dependent
359 on aerosol pH with significant mass transfer occurring at higher pH values, but a review
360 of past observations by Faloona [2009] suggests that supermicron, or coarse, SSA have
361 neutral to slightly alkaline pH while submicron aerosols are very acidic. Observations
362 from PASE allowed Faloona et al. [2009] to estimate aerosol mass transfer rates to course
363 SSA of 5-10% hr^{-1} at night and an average daytime loss of 5% hr^{-1}. Thus SSA uptake of
364 SO_2 may be on the order of homogeneous reactions with OH, but remains dependent on
365 aerosol pH such that rates vary from 0 and 10% based on atmospheric variability. Given
366 the height of the Kīlauea vents and prevailing wind patterns this pathway may be
367 important during high wind events, when coarse mode SSA are lofted high in the
368 boundary layer, or when the plume descends down to sea level.
369 When SO_2 dissolves in water it forms a weak acid that undergoes two
370 dissociations to form a total of three species, $HSO_3^-, H_2O \cdot SO_2, SO_3^{2-}$, the sum of which
371 are known collectively as S_{IV}. The solubility of SO_2 is a function of temperature and pH
372 of the solution. At pH 2-7, S_{IV} is almost entirely in the form of the bisulfite ion (HSO_3^-)
373 [Seinfeld and Pandis, 1998]. At lower temperatures there will be higher solubility. The
374 reaction rate will decrease with decreasing temperature, however, the increased reactant
375 concentration will tend to counterbalance the decreased reaction rate [Eatough et al.,
376 1994].
377 Hydrogen peroxide (H_2O_2) and ozone (O_3) are the most likely oxidants for SO_2 in
378 the aqueous phase. However, ozone reactions are highly pH dependent and only become
379 the leading oxidant at pH > 5.5 [Hegg, 1989; Seinfeld and Pandis, 1998]. Hydrogen

peroxide reactions are relatively independent of pH between pH 2-6. The pH of atmospheric water droplets reported is typically 3-6 [Eatough et al., 1994]. Rainwater samples taken in Hawai‘i yield an average pH = 4.5 [Miller and Yoshinaga, 1981] while Siegel et al. [1990] found 84% of rain samples downwind of Kīlauea had pH values less than 5.0. The large particle size of rain droplets relative to cloud droplets suggests that the pH of the smaller volume cloud droplets will likely be even lower and that the pH of rain droplets represents an upper limit. This suggests that hydrogen peroxide is the leading oxidant of sulfur dioxide in the aqueous phase in the vicinity of Kīlauea. Hydrogen peroxide, like the hydroxyl radical, is produced photochemically, both in the gas phase and aqueous phase [Warneck, 1999]. The average concentration of hydrogen peroxide found during the Pacific Atmospheric Sulfur Experiment (PASE) was 1.0 ppb [Simpson, 2010]. PASE was designed to study the chemistry in the trade wind regime that may influence cloud droplet chemistry and aerosol concentrations and composition [Bandy et al., 2011].

In order for the aqueous phase reaction to occur, both sulfur dioxide and hydrogen peroxide gases must be dissolved in cloud water. Hydrogen peroxide is considered highly soluble and sulfur dioxide moderately soluble. Equilibrium between the gas and aqueous phase concentrations is reached on very short time scales relative to droplet lifetime so that equilibrium can be considered. This allows the use of Henry's Law constants to determine aqueous phase concentrations. Henry's Law has a strong dependence on temperature. This dependence has been found by Huang and Chen [2010] for hydrogen peroxide and can be expressed as

$$K_H[\mathrm{H2O2}] = exp\left(\frac{a}{T} - b\right) \quad (10)$$

where a =7024 ± 138 and b = 11.97 ± 0.48 and T (K) is the equilibrium temperature. Huang and Chen [2010] showed that this relation is relatively independent of solution pH in the range of 1 to 7. This relationship results in $K_H[H_2O_2] = 1.08 \times 10^5$ M atm^{-1} at 25°C [Huang and Chen, 2010], where M, molarity, is the concentration of solute in solution expressed as 1 mol L^{-1} or 1 x 10^{-3} mol cm^{-3}. The recommended value of $K_H[H_2O_2]$ by the JPL is 8.44 x 10^4 M atm^{-1} (for 278 K < T < 303 K) with temperature dependence values for a = 7600 and b = 14.16 [Sander et al., 2011]. The recommended value for $K_H[SO_2]$ from JPL is 1.36 M atm^{-1} and the temperature dependence is given by

$$K_H[\mathrm{SO2}] = exp\left(\frac{a}{T} - b + cT\right) \tag{11}$$

where a = 4250, b = 39.72, and c = 4.525 [Sander et al., 2011]. The uncertainty in K_H is given as 10 to 50%.

The aqueous phase reaction of sulfur dioxide and hydrogen peroxide is expressed by Hoffman and Calvert [1985] as

$$-\frac{d[\mathrm{S_{IV}}]}{dt} = \frac{k[\mathrm{H^+}][\mathrm{H_2O_2}][\mathrm{HSO_3^-}]}{1 + K[\mathrm{H^+}]} \tag{12}$$

where the reaction constant, k = 7.45x 10^7 M^{-2} s^{-1}, K = 13 M^{-1} at 298 K. $[HSO_3^-]$ = $[SO_2](aq)K_s/H^+$ because it is assumed that most dissolved SO_2 is in the form of bisulfite, where K_s is the dissociation constant of $SO_2.H_2O$ = 1.3 x 10^{-2} M and the concentration of the hydrogen ion, [H$^+$], is the estimate of water droplet pH. Martin and Damschen [1981] provide another popular estimate of k = 5.2 x 10^6 M^{-2} s^{-1}. A pH of 4.5 is assumed here, which corresponds to an H$^+$ concentration of 3.16 x 10^{-5} M. Given this pH value and that the reaction is relatively independent of pH, the denominator is approximately 1, and equation (12) becomes

$$-\frac{d([SO_2](aq))}{dt} = k[H^+][H_2O_2][SO_2](aq) \quad (13)$$

where k = 9.1 (± 0.5) x 10^7 M^{-2} s^{-1} as proposed by Maass et al. [1999]. Caffrey et al. [2001] found this kinetic relation to work best for their modeling of cloud particle growth. If we assume 100% conversion efficiency to sulfate aerosol, equation (13) can be treated as an aerosol production equation by changing the left hand term to

$$\frac{d([SO_4](aq))}{dt} = k[H^+][H_2O_2][SO_2](aq) \quad (14)$$

Overnight observations at HAVO-OB on 20 July 2014 are used to estimate aqueous phase conversion rates because RH = 100% during this period. K_H values are corrected for pressure (altitude) using the 2014 annual mean station pressure from HAVO-OB. Values calculated from equations (10) and (11) at a temperature = 290.35 K and p = 0.867 atm are $K_H[H_2O_2]$ = 1.78 x 10^5 M atm^{-1} and $K_H[SO_2]$ = 1.55 M atm^{-1} for hydrogen peroxide and sulfur dioxide, respectively. When multiplied by the gas concentrations for H_2O_2 (1 x 10^{-9} atm^{-1}) and SO_2 (1 x 10^{-8} atm^{-1}) the aqueous phase concentrations are 1.78 x 10^{-4} M and 6.37 x 10^{-6} M, respectively.

Note that the SO_2 gas ($[SO_2](g)$) concentration is an order of magnitude greater than $[H_2O_2](g)$, but the solubility of H_2O_2 results in dissolved concentrations of $[H_2O_2](aq)$ four magnitudes greater than $[SO_2](aq)$. Thus, $[SO_2](aq)$ concentrations will be lower than $[H_2O_2](aq)$ initially, however, higher $[SO_2](g)$ concentrations will continue to dissolve and react with $[H_2O_2](aq)$ and ultimately $[H_2O_2](g)$ will be the limiting reactant. Using the rate coefficient, k = 9.1 x 10^7 M^{-2} s^{-1}, provided by Maass et al. [1999] the loss rate of $[SO_2](aq)$ is 3.26 x 10^{-6} M s^{-1}, or roughly a 50% decrease in $[SO_2](aq)$ per second. This rate is similar in magnitude to past theoretical conversion rates found by

442 Seinfeld and Pandis [1998] (Figure 4). Such rapid conversion assumed a homogeneous
443 H_2O_2 concentration within the cloud, however the reaction will likely be limited by
444 mixing of the SO_2 plume into and within.

445 This reaction is known to be very fast and should deplete all H_2O_2 within a matter
446 of minutes, which is the typical residence time of an air parcel in-cloud. Measurements
447 by Daum et al. [1984] suggest that both reactants rarely coexist in clouds or fog. Further
448 evidence in measurements by Barth et al. [1989] reveal that aqueous concentrations of
449 hydrogen peroxide are always below those expected in equilibrium from Henry's Law.
450 This suggests that the sulfur dioxide sink is removing hydrogen peroxide faster than it
451 can be replaced.

452 Simpson [2010] took three approaches to estimate in-cloud oxidation of SO_2
453 to sulfate aerosols using project-averaged values from the Pacific Atmospheric
454 Sulfur Experiment (PASE) conducted in 2007. Using chemical kinetic theory, the
455 amount of SO_2 oxidized during a single cloud encounter lasting 7 minutes (based on
456 updraft velocities below cloud and assuming a 500 m deep cloud) is 50 ± 30%. The
457 ratio of dimethyl sulfide to SO_2 during individual cloud encounters is used to
458 approximate the consumption of SO_2 using method two. Again the loss rate is found
459 to be 50 ± 30%. The third approach estimates conversion with a sulfur flux budget.
460 This method suggests 33-46% total SO_2 is consumed to produce 45-80% of the total
461 sulfate. It is important to note that SO_2 concentrations during PASE are between 1-
462 100 ppt, significantly lower than concentrations in the vicinity of Kīlauea.

463 In light of past observations and estimates of Simpson [2010] it is important to
464 assess the uncertainty in the reaction rate calculated here because a significant depletion
465 of H_2O_2 will make reactions between SO_2 and other reactants increasingly important.
466 Much of the uncertainty associated with the aqueous phase reaction of SO_2 with
467 H_2O_2 stems from the uncertainty in the temperature dependence of the Henry's Law
468 constants and the conversion rate coefficients. The uncertainty for $K_H[SO_2]$ is
469 approximately 50% [Sander et al., 2011] while $K_H[H_2O_2]$ is less than 1% (1.76 (± 0.01) x
470 10^5 M atm^{-1}). Because the reaction is limited by H_2O_2 concentrations, any error resulting
471 from uncertainty in SO_2 solubility is negligible. Estimates of k range from 5.2 x 10^6 M^{-2}
472 s^{-1} to 9.6 x 10^7 M^{-2} s^{-1}. By using the lower bound $[SO_2](aq)$ loss will be 3% per second,
473 or roughly a factor of 17.5 less than the upper bound estimate. While this lower
474 conversion rate will deplete H_2O_2 more slower, estimates from Hua et al. [2008] suggest
475 H_2O_2 production peaks at less than 1 ppb h^{-1}, meaning that over time (especially
476 overnight) H_2O_2 may still be depleted. The lower bound estimates are closer to those of
477 Simpson [2010] and differ in proportion to $[SO_2]$ used in the calculations.
478 If the rate of H_2O_2 production cannot keep pace with removal through aqueous
479 SO_2 reactions then secondary reaction pathways will become important. Although O_3
480 reactions are more dependent on solution pH, this pathway remains important at pH 3-6
481 should H_2O_2 be absent in significant concentrations [Eatough et al., 1994]. Ozone
482 concentrations in the marine boundary layer are higher than H_2O_2, with mean
483 concentrations between 15 - 19 ppb, and it is moderately soluble with a Henry's Law
484 coefficient of 1.3 x 10^{-2} M. The O_3 rate expression is given as

$$-\frac{d[\mathrm{S_{IV}}]}{dt} = (k_0[\mathrm{SO_2 \cdot H_2O}] + k_1[\mathrm{HSO_3^-}] + k_2[\mathrm{SO_3^{2-}}])[\mathrm{O_3(aq)}] \quad (15)$$

where k_0 = 2.4 x 10^4 M^{-1} s^{-1}, k_1 = 3.7 x 10^5 M^{-1} s^{-1}, and k_2 = 1.5 x 10^9 M^{-1} s^{-1} [Hoffman and Calvert, 1985], however, if all H_2O_2 is consumed in reactions with SO_2 then solution pH can easily drop below 3 making this reaction negligible. Additionally, the depletion of O_3 within volcanic plumes [Vance et al., 2010; Oppenheimer et al., 2010; Schuman et al., 2011; Kelly et al., 2013; Surl et al., 2015] will limit the impact of this pathway.

Emission estimates from Halema‘uma‘u Crater by Mather et al. [2012] show traces of Fe and Mn are being emitted, making conversion catalyzed via the Fe(III) and Mn(II) pathways possible. Mn is highly soluble and Fe is not water-soluble but would dissolve in an acidic solution such as H_2SO_4 so it is realistic to assume all Fe is dissolved in a cloud also impacted by the SO_2 laden volcanic. These reactants may be important conversion mechanisms near Halema‘uma‘u Crater from pH 3.5 to 6 (c.f. figure 6.25 in Seinfeld and Pandis, 1998). The rate expressions are given as

$$-\frac{d[\mathrm{S_{IV}}]}{dt} = k_{Fe}[\mathrm{Fe(III)}][\mathrm{SO_3^{2-}}] \quad (16)$$

$$-\frac{d[\mathrm{S_{IV}}]}{dt} = k_{Mn}[Mn(II)][S_{IV}] \quad (17)$$

where k_{Fe} = 1.2 x 10^6 M^{-1} s^{-1} for pH ≤ 5 [Hoffman and Calvert, 1985] and k_{Mn} = 1000 M^{-1} s^{-1} [Martin and Hill, 1987]. Fe and Mn emissions are estimated by Mather et al. [2012] as Fe/SO_2 = 7.7 x 10^{-5} and Mn/SO_2 = 1.4 x 10^{-6}. Given an SO_2 emission rate of 3000 t d^{-1} this amounts to Fe emission of 0.231 t d^{-1} and Mn emission of 4.2 x 10^{-3} t d^{-1}. Benitez-Nelson et al. (2003) measured Fe concentrations in cloud water near the volcano as 1 x 10^{-6} M and Sansone et al. (2002) estimated the Mn/Fe ratio near the volcano as 0.02. If all this Fe and Mn mass is dissolved in cloud water at a pH=4.5, then the reaction rates

504 for Fe(III) = 1.6 x 10^{-8} M s^{-1} and Mn(II) = 1.2 x 10^{-10} M s^{-1}. The reaction with Mn can be
505 neglected because of its magnitude but the reaction rate with Fe is secondary only to
506 H_2O_2 at pH < 5.5. Figure 4 shows the Fe reaction is highly dependent on solution pH
507 suggesting such high conversion rates due to Fe may be unrealistic given the low pH of
508 Hawaiian rainfall and implied lower pH of cloud water. However, given the relatively
509 high emission rate of Fe, this reaction may be important near the vent when H_2O_2 could
510 potentially be drawn down through SO_2 oxidation, especially in the presence of clouds or
511 fog at the summit of Kīlauea. As the plume moves downwind and disperses, H_2O_2
512 removal through SO_2 oxidation will decrease meaning the likelihood that Fe reactions
513 increasing in importance will remain low even though little to no Fe is being removed
514 from the plume.

515 Seinfeld and Pandis (1998) mention a synergism between Fe and Mn that can
516 increase reaction rates 3 to 10 times higher at low pH than would be predicted from the
517 sum. The results of this calculation are uncertain however they are included in figure 4
518 for completeness. Also included in figure 4 is oxidation by NO_2. This pathway is pH
519 dependent and due to low NO_2 concentrations around Hawaii (5 ppt) this reaction would
520 have a negligible impact on SO_2. For details of the NO_2 reaction see Seinfeld and Pandis
521 (1998).

522 A further mechanism for SO_2 oxidation in solution with sea salt is proposed via
523 halogen compounds HOCl and HOBr [Vogt et al., 1996]. The reactions are described by
524 Fogelman et al. (1989) and Troy and Margerum (1991) as follows

$$S_{(IV)} + HOCl \rightarrow S_{(VI)} + HCl \quad (18)$$

$$S_{(IV)} + HOBr \rightarrow S_{(VI)} + HBr \quad (19)$$

525 Simulations by Keene et al. [1998] found reactions with HOCl to be more rapid than
526 H_2O_2 at pH 3 – 5.5 and HOBr more rapid than H_2O_2 at pH > 5.5. The HOCl estimate is
527 highly uncertain since the rate constant is unknown but was assumed to be equal to that
528 of SO_3^{2-} [Alexander et al., 2012].

529 Von Glasow et al. [2002] extended the work of Vogt et al. [1996] to account for
530 SO_2 oxidation in aqueous solutions. They found that HOCl could be responsible for 5-
531 10% of aqueous sulfate formation as a result of reactions with S(IV) and sea salt (high
532 pH) in the remote marine boundary layer (MBL) while HOBr was responsible for 20-
533 30% sulfate formation, with a majority forming in cloud water. It is important to note that
534 estimates of Henry's Law constants for HOBr are a source of uncertainty, ranging from
535 93 M atm^{-1} [Vogt et al., 1996] to 6100 M atm^{-1} [Frenzel et al., 1998] and von Glasow et
536 al. [2002] used the value of Vogt et al. [1996].

537 Though initial calculations assumed these reactions were occurring the remote
538 MBL subsequent research has revealed halogens in volcanic plumes at concentrations
539 much higher than background levels. HOCl precursor OClO has been detected in
540 volcanic plumes [Bobrowski et al., 2007], and ClO has been reported as well [Lee et al.,
541 2005]. Horrocks et al. [2003] and Aiuppa et al. [2007] found little evidence of HOCl SO_2
542 reactions in volcanic plumes due to limitations related to high acidity of cloud droplets
543 and low background humidity.

544 HBr is a main volcanic emission compound and measurements of BrO in volcanic
545 plumes [Bani et al., 2009; Bobrowski et al., 2003, 2015; Bobrowski and Platt, 2007;
546 Boichu et al., 2011; Heue et al., 2011; Hörmann et al., 2013; Kelly et al., 2013; Kern et
547 al., 2009; Lee et al., 2005; Oppenheimer et al., 2006; Theys, et al., 2009] imply limits of

548 HOBr concentrations in-plume. Concentrations of HOBr are also implied through
549 observed O_3 depletion in volcanic plumes [Vance et al., 2010; Oppenheimer et al., 2010;
550 Surl et al., 2015; Zerefos et al., 2006] since aqueous HOBr is a required reactant in the
551 'bromine explosion' reaction chain to form BrO as detailed in [Bobrowski et al., 2003].
552 The formation of sulfate via HOBr appears to be an important pathway, but may
553 be limited due to the low pH (< 5) in Hawai'i (particularly in the volcanic plume itself).
554 Results of Keene et al. [1998] and von Glasow et al. [2002] suggest the reaction is highly
555 dependent on pH but even at pH=4.5, it may account for ~25% sulfate formation. With
556 the uncertainty around Henry's Law constant for HOBr, this reaction could be faster and
557 even match that of H_2O_2. Von Glasow et al. [2002] also found little sulfate formation (<
558 10%) from HOCl under low pH values. Further research is needed to determine the
559 magnitude of reactions in halogens and sulfur dioxide laden volcanic plumes.
560
561 **4. Summary**
562 Theoretical estimates of gas and aqueous phase oxidation of SO_2 at Kīlauea
563 Volcano have been evaluated and the results suggest that hydroxyl radical and hydrogen
564 peroxide are the dominant reaction pathways. For a frequently observed ground-level
565 SO_2 concentration (10 ppb) the range of conversion rates for the hydroxyl radical and
566 hydrogen peroxide reaction pathways are estimated from kinetic theory, where the range
567 is representative of the uncertainty associated with the temperature and moisture
568 dependence of the reactions. The estimated conversion rates represent results based on a
569 single reactant concentration. Given that SO_2 is the limiting reactant (except near the

570 source area) the amount of sulfate aerosols formed via reactions can increase given
571 higher SO_2 concentrations or decrease given lower SO_2 concentrations.
572 Oxidation of SO_2 in the gas phase is dominated by reactions with the hydroxyl
573 radical, OH. Reaction rates are estimated for daytime and nighttime conditions observed
574 at the Hawai‘i Volcanoes Observatory. Daytime rates range from 0.8 to 5% h^{-1} and
575 nighttime rates range from 0.01 to 0.07% h^{-1}. Because OH concentrations and production
576 peak during the day and production ceases overnight, a diurnal signal is expected.
577 Uncertainty in the conversion rate is addressed through the temperature and moisture
578 dependence of the reaction is represented through a reaction coefficient, k. Additional
579 uncertainty is the reaction rate results from concentrations of OH. Ozone depletion
580 within volcanic plumes has been well documented [Jourdain et al., 2016 and references
581 within], which reduces the formation of OH by as much as 30%. Under most
582 circumstances the limiting agent will be SO_2, however, near Halema‘uma‘u Crater the
583 SO_2 concentrations can exceed 100 ppm. Under such conditions OH would be
584 completely depleted through reactions with SO_2 and will be the limiting agent. This
585 reaction limit is reached with SO_2 concentrations as low as 10 ppm, however,
586 concentrations of this magnitude are not common beyond a few kilometers downwind
587 from the source.
588 The aqueous phase oxidation of SO_2 is dominated by reaction with hydrogen
589 peroxide, H_2O_2. This is because of the independence of the reaction on solution pH and
590 low ozone concentrations in the Central Pacific. Past observations of rainfall pH in
591 Hawai‘i suggest a range of pH values between 3 and 5.5, which is likely an upper bound.
592 Estimated reaction rates suggest a conversion rate of dissolved SO_2 between 3-50% s^{-1}.

593 Such a rapid reaction coupled with a rapid diffusion process is unsustainable over long
594 periods of time and will quickly lead to the depletion of the limiting reactant. Given that
595 parcels of air spend no more than a few minutes in shallow marine cumulus clouds
596 [Simpson 2010] and the observations of Daum et al. [1984] and Barth et al. [1989], the
597 reaction estimate here is limited by the ambient H_2O_2 concentrations (1.0 ppb) and H_2O_2
598 production, which has been estimated by Martin et al. [1997] to be 0.85 ppb d^{-1}. Thus for
599 an air parcel penetrating a cloud with 10 ppb SO_2 and 1 ppb H_2O_2, the maximum loss of
600 SO_2 through conversion to SO_4 is 1 ppb or 10%.
601 Other aqueous phase reactions via O_3, Fe(III), and Mn(II), HOBr, and HOCl were
602 considered to assess if the associated conversion rates are significant relative to H_2O_2.
603 Ozone reactions are highly pH dependent and become important only in the event that
604 H_2O_2 is drawn down first. A reduction in H_2O_2 via reaction with SO_2 will produce
605 sulfuric acid, H_2SO_4, reducing solution pH limiting any contribution from O_3. Observed
606 ozone depletion within volcanic plumes [Surl et al., 2015] further suggests this
607 mechanism is negligible. Fe and Mn are emitted from Halemaʻumaʻu [Mather et al.,
608 2012] and were measured by Sansone et al. [2002] and Benitez-Nelson et al. [2003].
609 Measured concentrations and reaction kinetics for Fe(III) and Mn(II) suggest that
610 catalyzed reactions with Mn(II) are negligible, whereas Fe(III) could be important should
611 H_2O_2 be depleted. The importance of this reaction is limited to the region around the
612 vents because of low Fe emission rates, however periods of clouds near the summit of
613 Kīlauea can increase the significance of this rapid reaction rate. There is much
614 uncertainty about the reaction rates of HOBr and HOCl but simulations suggest that
615 HOBr may play as an important role as Fe(III) whereas HOCl is limited by pH.

Limits in both reaction rates theoretically exist based on environmental factors (i.e. temperature, relative humidity, solar insolation), emission rates, and ambient reactant concentrations. The oxidation of SO_2 from Kīlauea is dominated by the hydroxyl radical in the gas phase and hydrogen peroxide in the aqueous phase. Given high SO_2 emissions from the summit vent at Halema‘uma‘u Crater, the oxidation by these reactants may become limited by their modest ambient concentrations. Under such circumstances secondary reactions may become important, such as Fe(III) or HOBr for aqueous conversion. However these circumstances are limited to SO_2 concentrations $\geq$ 10 ppm and high concentrations of Fe that are typically only found close to the emission source.

The importance of the gas-phase reaction to ground level concentrations of both SO_2 and SO_4 is paramount to improving forecasts downwind of Kīlauea Volcano. For kilometers downwind the volcanic plume can often be observed traveling at or just above the ground under stable conditions. Ground level clouds are only occur near the summit of Kīlauea over of period of hours making the relative contribution of aqueous phase reactions to ground level concentrations minor over the course of the year. Gas phase oxidation via OH is expected in the range of 0.8 to 5% h^{-1}. Theoretical estimates of in-cloud conversion are not as straight forward as gas-phase conversion. Oxidation via H_2O_2 is limited in-cloud by ambient concentrations but can reach 100% for SO_2 gas concentrations < H_2O_2 gas concentrations.

5. Acknowledgements

637 This research was supported by NOAA under Grant NA11NMF4320128, NSF under
638 Grant number 1108569, and ONR Award N00014-18-1-2166. Data were obtained from
639 the National Park Service and NASA's Global Tropospheric Experiment archive.
640

641 **6. References**

642 Aiuppa, A., A. Franco, R. von Glasow, A. G. Allen, W. D. Alessandro, T. A. Mather, D.
643 M. Pyle, and M. Valenza, 2007, The tropospheric processing of acidic gases and
644 hydrogen sulphide in volcanic gas plumes as inferred from field and model
645 investigations, *Atmos. Chem. Phys.*, **7,** 1441-1450, doi:10.5194/acp-7-1441-2007.
646 Alexander, B., D. J. Allman, H. M. Amos, T. D. Fairlie, J. Dachs, D. A. Hegg, and R. S.
647 Sletten, 2012, Isotopic constraints on the formation pathways of sulfate aerosol in
648 the marine boundary layer in the subtropical northeast Atlantic Ocean, *J. Geophys.*
649 *Res.*, **117,** D06304, doi:10.1029/2011JD016773.
650 Atkinson, R., D. L. Baulch, R. A. Cox, R. F. Hampson Jr., J. A. Kerr, and J. Troe, 1989,
651 Evaluated kinetic and photochemical data for atmospheric chemistry: Supplement
652 III, *J. Phys. Chem. Ref. Data***, 18(2),** 881-1,097.
653 Bandy, A., I. C. Faloona, B. W. Blomquist, B. J. Huebert, A. D. Clarke, S. G. Howell, R.
654 L. Mauldin, C. A. Cantrell, J. G. Hudson, B. G. Heikes, J. T. Merrill, Y. Wang, D.
655 W. O'Sullivan, W. Nadler, and D. D. Davis, 2011, Pacific atmospheric sulfur
656 experiment (PASE): dynamics and chemistry of the south Pacific tropical trade wind
657 regime, *J. Atmos. Chem.*, **68**, 5-25, https://doi.org/10.1007/s10874-012-9215-8.

658 Bani, P., C. Oppenheimer, V. I. Tsanev, S. A. Carn, S. J. Cronin, R. Crimp, J. A. Calkins,
659 D. Charley, M. Lardy, and T. R. Roberts, 2009, Surge in sulphur and halogen
660 degassing from Ambrym volcano, Vanuatu, *B. Volcanol*., **71**, 1159–1168.
661 Barth, M. C., D. A. Hegg, P. V. Hobbs, J. G. Walega, G. L. Kok, B. G. Heikes, and A. L.
662 Lazrus, 1989, Measurements of atmospheric gas-phase and aqueous-phase
663 hydrogen peroxide concentrations in winter on the east coast of the United
664 States, *Tellus*, **41B**, 61-69.
665 Baulch, D. L., R. A. Cox, R. F. Hampson, Jr., J. A. Kerr, J. Troe, and R. T. Watson, 1980,
666 Evaluated kinetic and photochemical data for atmospheric chemistry, *J. Phys.*
667 *Chem. Ref. Data*, **9**, 295-471.
668 Bobrowski, N. and U. Platt, 2007, SO_2 = BrO ratios studied in five volcanic plumes, *J.*
669 *Volcanol. Geoth. Res.*, **166**, 147–160, 2007.
670 Bobrowski, N., G. Hönninger, B. Galle, and U. Platt, 2003, Detection of bromine
671 monoxide in a volcanic plume, *Nature*, **423**, 273–276.
672 Bobrowski, N., R. von Glasow, A. Aiuppa, S. Inguaggiato, I. Louban, O. W. Ibrahim, and
673 U. Platt, 2007, Reactive halogen chemistry in volcanic plumes, *J. Geophys. Res.*,
674 **112**, D06311, doi:10.1029/2006JD007206.
675 Bobrowski, N., R. von Glasow, G. B. Giuffrida, D. Tedesco, A. Aiuppa, M. Yalire, S.
676 Arellano, M. Johansson, and B. Galle, 2015, Gas emission strength and evolution
677 of the molar ratio of BrO = SO_2 in the plume of Nyiragongo in comparison to
678 Etna, *J. Geophys. Res.-Atmos.*, **120**, 277–291.

679 Boichu, M., C. Oppenheimer, T. J. Roberts, V. Tsanev, and P. R. Kyle, 2011, On
680 bromine, nitrogen oxides and ozone depletion in the tropospheric plume of
681 Erebus volcano (Antarctica), *Atmos. Environ.*, **45**, 3856–3866.
682 Brown, S. S. and J. Stutz, 2012, Nighttime radical observations and chemistry, *Chem.*
683 *Soc. Rev.*, **41**, 6405-6447, doi:10.1039/c2cs35181a.
684 Buckholder, J. B., S. P. Sander, J. Abbatt, J. R. Barker, R. E. Huie, C. E. Kolb, M. J. Kurylo,
685 V. L. Orkin, D. M. Wilmouth, and P. H. Wine, 2015, Chemical kinetics and
686 photochemical data for use in atmospheric studies, evaluation No. 18, JPL
687 Publication 15-10, Jet Propulsion Laboratory, Pasadena,
688 http://jpldataeval.jpl.nasa.gov.
689 Caffrey, P., W. Hoppel, G. Frick, L. Pasternack, J. Fitzgerald, D. Hegg, S. Gao, R. Leaitch,
690 N. Shantz, T. Albrechcinski, and J. Ambrusko, 2001, In-cloud oxidation of SO_2 by
691 O_3 and H_2O_2: Cloud chamber measurements and modeling of particle growth, *J.*
692 *Geophys. Res.*, **106**, D21, 27,587-27,601.
693 Daum, P. H., R. J. Kelly, S. E. Schwartz, L. Newman, 1984, Measurements of the
694 chemical composition of stratiform clouds, *Atmos. Environ.,* **18**, 2,671-2,684.
695 Eatough, D. J., R. J. Arthur, N. L. Eatough, M. W. Hill, N. F. Mangelson, B. E. Richter, and
696 L. D. Hansen, 1984, Rapid conversion of SO_2(g) to sulfate in a fog bank, *Environ.*
697 *Sci. Technol.*, **18**, 855-859.
698 Eatough, D. J., F. M. Caka, and R. J. Farber, 1994, The conversion of SO_2 to sulfate in
699 the atmosphere, *Isr. J. Chem.,* **34**, 301-314.
700 Elias, T. and A. J. Sutton, 2007, Sulfur dioxide emission rates from Kīlauea Volcano,
701 Hawai‘i, an update: 2002-2006, U.S. Geol. Survey. Open-File Rep. 2007-1114.

Elias, T. and A. J. Sutton, 2012, Sulfur dioxide emission rates from Kīlauea Volcano, Hawai‘i, 2007-2010, U.S. Geol. Survey. Open-File Rep. 2012-1107.

Environmental Integrity Project, 26 July 2007, Dirty kilowatts: America's most polluting power plants, Environmental Integrity Project, Washington D.C.

ESPERE, 2006, ESPERE Climate Encyclopedia. Accessed 23 March 2016. [Available online at http://klimat.czn.uj.edu.pl/enid/Service/Encyclopaedia_4sl.html.

Faloona, I., 2009, Sulfur processing in the marine atmospheric boundary layer: A review and critical assessment of modeling uncertainties, *Atmos. Environ.*, **43**, 2841-2854, doi:10.1016/j.atmosenv.2009.02.043.

Faloona, I, S. A. Conley, B. Blomquist, A. D. Clarke, V. Kapustin, S. Howell, D. H. Lenschow, A. R. Bandy, 2009, Sulfur dioxide in the tropical marine boundary layer: dry deposition and heterogeneous oxidation observed during the Pacific Atmospheric Sulfur Experiment, *J. Atmos. Chem.*, **63**, 13-32, doi:10.1007/s10874-010-9155-0.

Fogelman, K. D., D. M. Walker, and D. W. Margerum, 1989, Non-metal redox kinetics: hypochlorite and hypochlorous acid reactions with sulfite, *Inorg. Chem.*, **28**, 986-993.

Forberich, O., T. Pfeiffer, M. Spiekermann, J. Walter, F. J. Comes, R. Grigonis, K. C. Clemitshaw, and R. A. Burgess, 1999, Measurement of the diurnal variation of the OH radical concentration and analysis of the data by modeling, *J. Atmos. Chem.*, **33**, 155-181.

723 Frenzel, A., V. Scheer, R. Sikorski, Ch. George, W. Behnke, and C. Zetzsch, 1998,
724 Heterogeneous interconversion reactions of $BrNO_2$ $ClNO_2$, Br_2, and Cl_2, *J. Phys.*
725 *Chem. A*, **102**, 1329-1337, doi:10.1021/jp973044b.
726 Gauthier, P.-J., O Sigmarsson, M. Gouhier, B. Haddadi, and S. Moune, 2016, Elevated
727 gas flux and trace metal degassing from the 2014-2015 fissure eruption at the
728 Bárðarbunga volcanic system, Iceland, *J. Geophys. Res. Solid Earth*, **121**,
729 doi:10/1002/2015JB012111.
730 Hand, J. L., B. A. Schichtel, W. C. Malm, and M. L. Pitchford, 2012, Particulate sulfate
731 ion concentration and SO_2 emission trends in the United States from the early
732 1990s through 2010, *Atmos. Chem. Phys.,* **12**, 10,353-10,365, doi:10.5194/acp-
733 12-10353-2012.
734 Hand, T. M., C. Y. Chan, A. A. Mehrabzadeh, W. H. Pan, and R. J. O'Brien, 1991, Diurnal
735 cycle of tropospheric OH, *Nature*, **322**, 617-620.
736 Hawai'i Department of Health, 2013, Documentation for natural events excluded
737 data Kona air monitoring station, AQS ID 15-001-1012 2011-2012 $PM_{2.5}$
738 exceedances, State of Hawai'i Department of Health Clean Air Branch, Honolulu,
739 Hawai'i.
740 Hegg, D. A., 1989, The relative importance of major aqueous sulfate formation
741 reactions in the atmosphere, *Atmos. Res.*, **22**, 323-333.
742 Heue, K.-P., C. A. M. Brenninkmeijer, A. K. Baker, A. Rauthe-Schöch, D. Walter, T.
743 Wagner, C. Hörmann, H. Sihler, B. Dix, U. Friess, U. Platt, B. G. Martinsson, P. F. J.
744 van Velthoven, A. Zahn, and R. Ebinghaus, 2011, SO2 and BrO observation in the

plume of the Eyjafjallajökull volcano 2010: CARIBIC and GOME-2 retrievals, *Atmos. Chem. Phys.*, **11**, 2973-2989, doi:10.5194/acp-11-2973-2011.

Hoffman, M. R. and J. G. Calvert, 1985, Chemical transformation modules for Eulerian acid deposition models: Vol. II. The aqueous-phase chemistry, Acid Deposition Modeling Project, National Center for Atmospheric Research.

Holben, B. N., D. Tanre, A. Smirnov, T. F. Eck, I. Slutsker, N. Abuhassan, W. W. Newcomb, J. Schafer, B. Chatenet, F. Lavenue, Y. J. Kaufman, J. VandeCastle, A. Setzer, B. Markham, D. Clark, R. Frouin, R. Halthore, A. Karnieli, N. T. O'Neill, C. Pietras, R. T. Pinker, K. Voss, and G. Zibordi, 2001, An emerging ground-based aerosol climatology: Aerosol Optical Depth from AERONET, *J. Geophys. Res.,* **106,** D11, 12,067-12,097.

Hörmann, C., H. Sihler, N. Bobrowski, S. Beirle, M. Penning de Vries, U. Platt, U., and T. Wagner, 2012, Systematic investigation of bromine monoxide in volcanic plumes from space by using the GOME-2 instrument, *Atmos. Chem. Phys*., **13**, 4749–4781, doi:10.5194/acp-13-4749-2013.

Horrocks, L. A., C. Oppenheimer, M. R. Burton, and H. J. Duffell, 2003, Compositional variation in tropospheric volcanic gas plumes: evidence from ground-based remote sensing in volcanic degassing, eds. C. Oppenheimer, D. Pyle and J. Barclay, *Geological Society Special Publications*, **213**, 349-369.

Hua, W., Z. M. Chen, C. Y. Jie, Y. Kondo, A. Hofzumahaus, N. Takegawa, C. C. Chang, K. D. Lu, Y. Miyazaki, K. Kita, H. L. Wang, Y. H. Zhang, and M. Hu, 2008, Atmospheric hydrogen peroxide and organic hydroperoxides during PRIDE-PRD'06, China:

their concentrations, formation mechanism and contribution to secondary aerosols, *Atmos. Chem. Phys.*, **8**, 6755-6773.

Huang, D. and Z. Chen, 2010, Reinvestigation of the Henry's Law constant for hydrogen peroxide with temperature and acidity variation, *J. Environ. Sci.*, **22(4)**, 570-574.

Jourdain, L., T. J. Roberts, M. Pirre, and B. Josse, 2016, Modeling the reactive halogen plume from Ambrym and its impact on the troposphere with the CCATT-BRAMS mesoscale model, *Atmos. Chem. Phys.*, **16**, 12099-12125, doi:10.5194/acp-16-12099-2016.

Keene, W. C., R. Sander, A. A. P. Pszenny, R. Vogt, P. J. Crutzen, and J. N. Galloway, 1998, Aerosol pH in the marine boundary layer: a review and model evaluation, *J. Aerosol Sci.*, **29**, 339-356.

Kelly, P., Kern, C., Lopez, T., Werner, C., Roberts, T., Aiuppa, A., 2013, Rapid chemical evolution of tropospheric volcanic emissions from Redoubt Volcano, Alaska, based on observations of ozone and halogen-containing gases, *J. Volcanol. Geoth. Res.*, **259**, 317-333. doi.org/10.1016/j.jvolgeores.2012.04.023.

Kroll, J. H., E. S. Cross, J. F. Hunter, S. Pai, TREX XII, TREX XI, L. M. M. Wallace, P. L. Croteau, J. T. Jayne, D. R. Worsnop, C. L. Heald, J. G. Murphy, and S. L. Frankel, 2015, Atmospheric evolution of sulfur emissions from Kīlauea: Real-time measurements of oxidation, dilution, and neutralization within a volcanic plume, *Environ. Sci. Technol.*, **49(7)**, 4129-4137, doi:10.1021/es506119x.

Lee, C., Y. J. Kim, H. Tanimoto, N. Bobrowski, U. Platt, T. Mori, K. Yamamoto, and C. S. Hong, 2005, High ClO and ozone depletion observed in the plume of Sakurajima volcano, Japan, *Geophys. Res. Lett.*, **32**, L21809, doi:10.1029/2005GL023785.

Maass, F., H. Elias, and K. J. Wannowius, 1999, Kinetics of the oxidation of hydrogen sulfite by hydrogen peroxide in aqueous solution: Ionic strength effects and temperature dependence, *Atmos. Environ.*, **33**, 4,413-4,419.

Martin, D., M. Tsivou, B. Bonsang, C. Abonnel, T. Carsey, M. Springer-Young, A. Pszenny, and K. Suhre, 1997, Hydrogen peroxide in the marine atmospheric boundary layer during the Atlantic Stratocumulus Transition Experiment/Marine Aerosol and Gas Exchange experiment in the eastern subtropical North Atlantic, *J. Geophys. Res.*, 102(D5), 6003-6015, https://doi.org/10.1029/96JD03056.

Martin, L. R. and D. E. Damschen, 1981, Aqueous oxidation of sulfur-dioxide by hydrogen-peroxide at low pH, *Atmos. Environ.*, **15**, 1615-1621.

Martin, L. R. and M. W. Hill, 1987, The effect of ionic strength on the manganese catalyzed oxidation of sulfur(IV), *Atmos. Environ.*, **21**, 2267-2270.

Mather, T. A., M. L. I. Witt, D. M. Pyle, B. M. Quayle, A. Aiuppa, E. Bagnato, R. S. Martin, K. W. W. Sims, M. Edmonds, A. J. Sutton, and E. Elyinskaya, 2012, Halogens and trace metal emissions from the ongoing 2008 summit eruption of Kilauea volcano, Hawai'i, *Geochim. Cosmochim. Acta.*, **83**, 292-323.

Mauldin, R. L., F. L. Eisele, C. A. Cantrell, E. Kosciuch, B. A. Ridley, and B. Lefer, 2001, Measurements of OH aboard the NASA P-3 during PEM-Tropics B, *J. Geophys. Res.*, **106**, 32,657-32,666.

McGonigle, A. J. S., P. Delmelle, C. Oppenheimer, V. I. Tsanev, T. Delfosse, G. Williams-Jones, K. Horton, and T. A. Mather, 2004, SO_2 depletion in tropospheric volcanic plumes, *Geophys. Res. Lett.*, **31**, L13201, doi:10.1029/2004GL019990.

Miller, J. M. and A. M. Yoshinaga, 1981, The pH of Hawaiian precipitation a preliminary report, *Geophys. Res. Lett.*, **8**, 779-782.

Nadau, P. A., 2006, A multi-parameter investigation of volcanic plume behavior and resultant environmental impact at a persistently degassing volcano, Masaya, Nicaragua, M. S. Thesis, Dept. of Earth Sciences, Simon Fraser Univ., Burnaby, British Columbia, Canada.

Oppenheimer, C., P. Francis, and J. Stix, 1998, Depletion rates of sulfur dioxide in tropospheric volcanic plumes, *Geophys. Res. Lett.,* **25(14)**, 2,671-2,674.

Oppenheimer, C., V. I. Tsanev, C. F. Braban, R. A. Cox, J. W. Adams, A. Aiuppa, N. Bobrowski, P. Delmelle, J. Barclay, and A. J. S. McGonigle, 2006, BrO formation in volcanic plumes, *Geochim. Cosmochim. Ac.*, **70**, 2935–2941.

Oppenheimer, C., P. Kyle, F Eisele, J. Crawford, G. Huey, D. Tanner, S. Kim, L. Mauldin, D. Blake, A. Beyersdorf, M. Buhr, and D Davis, 2010, Atmospheric chemistry of an Antarctic volcanic plume, *J. Geophys. Res.*, **115**, D04303, doi:10.1029/2009/JD011910.

Perry, K. D., T. A. Cahill, R. C. Schnell, and J. M. Harris, 1999, Long-range transport of anthropogenic aerosols to the National Oceanic and Atmospheric Administration baseline station at Mauna Loa Observatory, Hawai‘i, *J. Geophys. Res.*, **104**, 18521-18533.

851 Porter, J. N., K. A. Horton, P. J. Mouginis-Mark, B. Lienert, S. K. Sharma, and E. Lau,
852 2002, Sun photometer and lidar measurements of the plume from the Hawai'i
853 Kīlauea Volcano Pu'u 'Ō'o vent: Aerosol flux and SO2 lifetime, *Geophys. Res.*
854 *Lett.*, **29(16)**, doi:10.1029/2002GL014744.
855 Raes, F., A. Saltelli, and R. Van Dingenen, 1992, Modeling formation and growth of
856 H_2SO_4-H_2O aerosols: Uncertainty analysis and experimental evaluation, *J.*
857 *Aerosol Sci.*, **23**, 759-771.
858 Rodriquez, L. A., I. M. Watson, V. Hards, G. Ryan, M. Edmonds, C. Oppenheimer, and
859 G. J. S. Bluth, 2005, SO_2 conversion rates at Soufrière Hills Volcano, Montserrat,
860 B. W. I. Paper presented at 17th Caribbean Geological Conference, San Juan,
861 Puerto Rico.
862 Rotstayn, L. D. and U. Lohmann, 2002, Simulation of the tropospheric sulfur cycle in
863 a global model with a physically based cloud scheme, *J. Geophys. Res.*, **107**, 4592,
864 doi:10.1029/2002JD002128.
865 Sander, S. P., J. Abbatt, J. R. Barker, J. B. Burkholder, R. R. Friedl, D. M. Golden, R. E.
866 Huie, C. E. Kolb, M. J. Kurylo, G. K. Moortgat, V. L. Orkin and P. H. Wine, 2011,
867 Chemical Kinetics and Photochemical Data for Use in Atmospheric Studies,
868 Evaluation No. 17, JPL Publication 10-6, Jet Propulsion Laboratory, Pasadena,
869 2011 http://jpldataeval.jpl.nasa.gov.
870 Schuman, U., B. Weinzierl, O. Reitebuch, H. Schlager, A. Minikin, C. Forster, R.
871 Baumann, T. Sailer, K. Graf, H. Mannstein, C. Voigt, S. Rahm, R. Simmer, M.
872 Scheibe, M. Lichtenstern, P. Stock, H. Rüba, D. Schäuble, A. Tafferner, M.
873 Rautenhaus, T. Gerz, H. Ziereis, M. Krautstrunk, C. Mallaun, J.-F. Gayet, K.

874 Leike, K. Kandler, M. Ebert, S. Weinbruch, A. Stohl, J. Gasteiger, S. Gross, V.
875 Freudenthaler, M. Weigner, A. Ansmann, M. Tesche, H. Olafsson, and K. Sturm,
876 2011, Airborne observations of the Eyjajalla volcano ah cloud over Europe
877 during air space closure in April and May 2010, *Atmos. Chem. Phys.*, **11**, 2245-
878 2279, doi:10.5194/acp-11-2245-2011.
879 Seinfeld, J. H. and S. N. Pandis, 1998, *Atmospheric Chemistry and Physics: From Air*
880 *Pollution to Climate Change*, John Wiley and Sons. Inc., New York.
881 Sharma, K., S. Blake, and S. Self, 2004, SO_2 emissions from basaltic eruptions, and the
882 excess sulfur issue, *Geophys. Res. Lett.*, **31**, L13612,
883 doi:10.1029/2004GL019688.
884 Shaw, G. E., 1980, Transport of Asian desert aerosol to the Hawaiian Islands, *J. App.*
885 *Meteorol.*, **19**, 1254-1259.
886 Singh, H. B., W. H. Brune, J. H. Crawford, F. Flocke, and D. J. Jacob, 2008, Chemistry
887 and transport of pollution over the Gulf of Mexico and the Pacific: Spring 2006
888 INTEX-B Campaign overview and first results, *Atmos. Chem. Phys.*, **9**, 2301-2318,
889 doi:10.5194/acp-9-2301-2009.
890 Siegel, B. Z., M. Nachbar-Hapai, and S. M. Siegel, 1990, The contribution of sulfate to
891 rainfall pH around Kilauea Volcano, Hawai'i, *Water Air Soil Poll.*, **52**, 227-235.
892 Simpson, R. M. C., 2010, Mechanisms of sulfate production in the remote equatorial
893 Pacific marine boundary layer, Master's Thesis, University of Hawai'i at Mānoa,
894 Honolulu, Hawai'i.

895 Surl, L., D. Donohue, A. Aiuppa, N. Bobrowski, and R. von Glasow, 2015,
896 Quantification of the depletion of ozone in the plume of Mount Etna, *Atmos.*
897 *Chem. Phys.*, **15**, 2613-2628, doi:10.5194/acp-15-2613-2015.
898 Troy, R. C. and D. W. Margerum, 1991, Non-metal redox kinetics: hypobromite and
899 hypobromous acid reactions with iodide and with sulfite and the hydrolysis of
900 bromosulfate, *Inorg. Chem.*, **30**, 3538-3543.
901 Theys, N., M. Van Roozendael, B. Dils, F. Hendrick, N. Hai, and M. De Mazière, 2009,
902 First satellite detection of volcanic bromine monoxide emission after the
903 Kasatochi eruption, *Geophys. Res. Lett.*, **36**, L03809,
904 doi:10.1029/2008GL036552.
905 Vance, A., A. J. S. McGonigle, A. Aiuppa, J. L. Stith, K. Turnbull, and R. Von Glasow,
906 2010, Ozone depletion in tropospheric volcanic plumes, *Geophys. Res. Lett.*, **37**,
907 L22802, doi:10.1029/2010GL044997.
908 Vogt, R., P. J. Crutzen and R. Sander, 1996, A mechanism for halogen release from
909 sea-salt aerosol in the remote marine boundary layer, *Nature*, **383**, 327-330.
910 Von Glasow, R., R. Sander, A. Bott, and P. J. Crutzen, 2002, Modeling halogen
911 chemistry in the marine boundary layer 2. Interactions with sulfur and the
912 cloud-covered MBL, *J. Geophys. Res.*, **107**, 4323, doi:10.1029/2001JD000943.
913 Warneck, P., 1999, The relative importance of various pathways for the oxidation of
914 sulfur dioxide and nitrogen dioxide in sunlit continental clouds, *Phys. Chem.*
915 *Chem. Phys.,* **1**, 5,471-5,483.
916 Zerefos, C. P Nastos, D. Balis, A. Papayannis, A. Kelepertsis, E. Kannelopoulou, D.
917 Nikolakis, C. Eleftheratos, W. Thomas, and C. Varotsos, 2006, A complex study of

Etna's volcanic plume from ground-based, *in situ* and space-borne observations, *Intern. J. Rem. Sens.*, **27**, 1855-1864, doi:10.1080/01431160500462154.

7. Tables

Table 1: Previously reported SO_2 loss rates reported from tropical volcanoes using correlation spectrometers.

Table 2: Potential gas-phase SO_2 reactions.

Table 3: Quantities used to calculate range of theoretical gaseous conversion rates.

Table 1: Previously reported SO_2 loss rates reported from tropical volcanoes using correlation spectrometers.

Site	SO_2 loss rate, k (s^{-1})	SO_2 loss rate, % h^{-1}	Reference
Masaya, Nicaragua	1±2e-5	0-10	McGonigle et al. [2004]
Soufrière Hills, Montserrat	1.5e-5 - 8.2e-4	5-95	Rodriguez et al. [2005]
Soufrière Hills, Montserrat	1.4e-3 - 5.4e-3	99.4 +	Oppenheimer et al. [1998]
Kīlauea, Hawai'i	1.9e-5 - 5.5e-5	7-18	Porter et al. [2002]
Kīlauea, Hawai'i	2.4e-6 – 5.3e-7	0.2-1.0	Kroll et al. [2015]

Table 2: Potential gas-phase SO_2 reactions. All values from Buckholder et al. [2015].

Reaction	k(298 K)
$OH + SO_2 \rightarrow HOSO_2$	1.6×10^{-12}
$O+SO_2 \rightarrow SO_3$	4.2×10^{-14}
$O_3 + SO_2 \rightarrow SO_3 + O_2$	$< 2.0 \times 10^{-22}$
$HO_2 + SO_2 \rightarrow$ products	$< 1.0 \times 10^{-18}$
$NO_2 + SO_2 \rightarrow$ products	$< 2.0 \times 10^{-26}$
$NO_3 + SO_2 \rightarrow$ products	$< 7.0 \times 10^{-21}$
$CH_3O2 + SO_2 \rightarrow$ products	$< 5.0 \times 10^{-17}$
$CH_2OO + SO_2 \rightarrow$ products	3.8×10^{-11}
anti-$CH_3CHOO + SO_2 \rightarrow$ products	2.2×10^{-10}
syn-$CH_3CHOO + SO_2 \rightarrow$ products	2.65×10^{-11}

$ClO + SO_2 \rightarrow Cl + SO_3$	$< 4.0 \times 10^{-18}$

930

931 **Table 3: Quantities used to calculate range of theoretical gaseous conversion rates.**

Quantity	Daytime	Nighttime
Temperature (°C)	21.9	17.1
Relative humidity (%)	79	100
SO_2 (molecules cm^{-3})	2.46×10^{11}	2.46×10^{11}
k (molecules cm^{-3} s^{-1})	5.58×10^{-13}	4.04×10^{-13}
OH (molecules cm^{-3})	1×10^{7}	2×10^{5}
Conversion rate (% h^{-1})	2	0.03
Conversion rate range (k uncertainty) (% h^{-1})	0.8-5	0.01-0.07

932

933 **8. Figures**

934 Figure 1: Days per year when EPA 1-hr SO_2 concentration exceeded the National

935 Ambient Air Quality Standard of 75 ppb. HOVE stands for Hawaiian Ocean View

936 Estates and HAVO OB stands for Hawai'i Volcanoes Observatory.

937 Figure 2: Concentrations of OH measured during INTEX-B flights. Blue dots

938 represent all 1-min averaged OH measurements and orange dots represent just

939 those collected below 3.0 km AGL. The black line represents the hourly averaged OH

940 values.

941 Figure 3: Estimated loss/production rate (s^{-1}) of OH calculated from INTEX-B CO,

942 CH4, and OH data.

943 Figure 4: Comparison of aqueous-phase oxidation paths near Kīlauea Volcano,

944 Hawai'i. The rate of conversion of S(IV) to S(VI) as a function of pH. Condition

945 assumed are: $[SO_2(g)]$ = 10 ppb; $[NO_2(g)]$ =5 ppt; $[H_2O_2(g)]$=1 ppb; $[O_3(g)]$ = 20 ppb;

946 [Fe(III)] = 1.0 μM; [Mn(II)]= 0.02 μM.

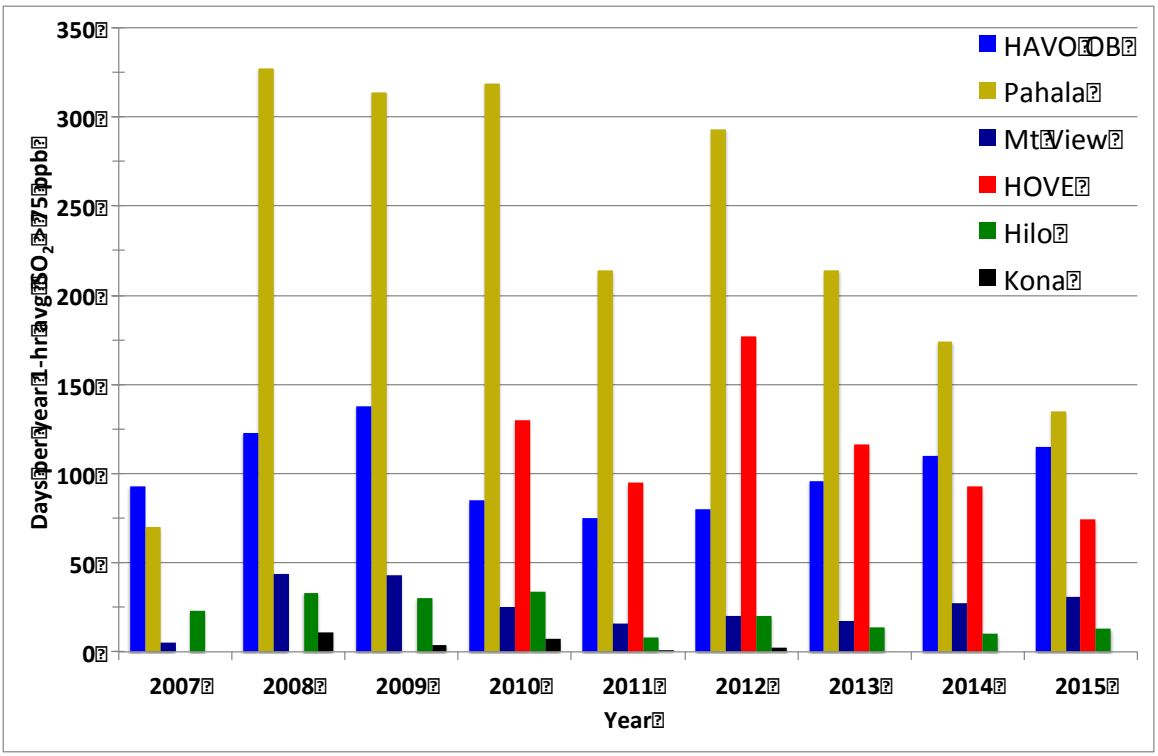

947

948 **Figure 1: Days per year when EPA 1-hr SO_2 concentration exceeded the National Ambient Air Quality**

949 **Standard of 75 ppb. HOVE stands for Hawaiian Ocean View Estates and HAVO OB stands for Hawai'i**

950 **Volcanoes Observatory.**

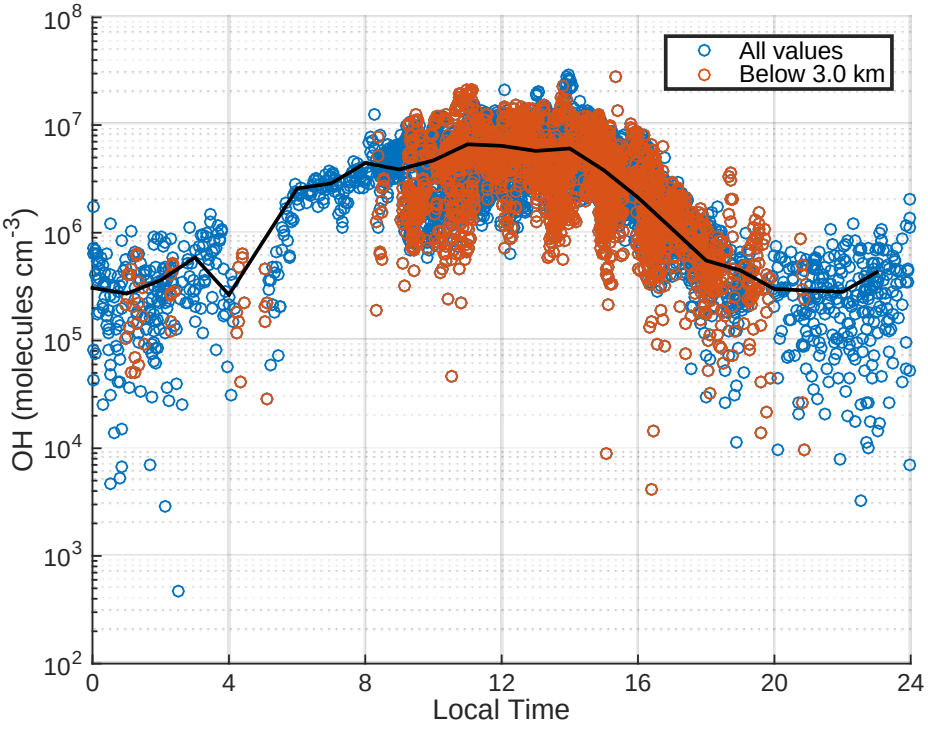

951

Figure 2: Concentrations of OH measured during INTEX-B flights. Blue dots represent all 1-min averaged OH measurements and orange dots represent just those collected below 3.0 km AGL. The black line represents the hourly averaged OH values.

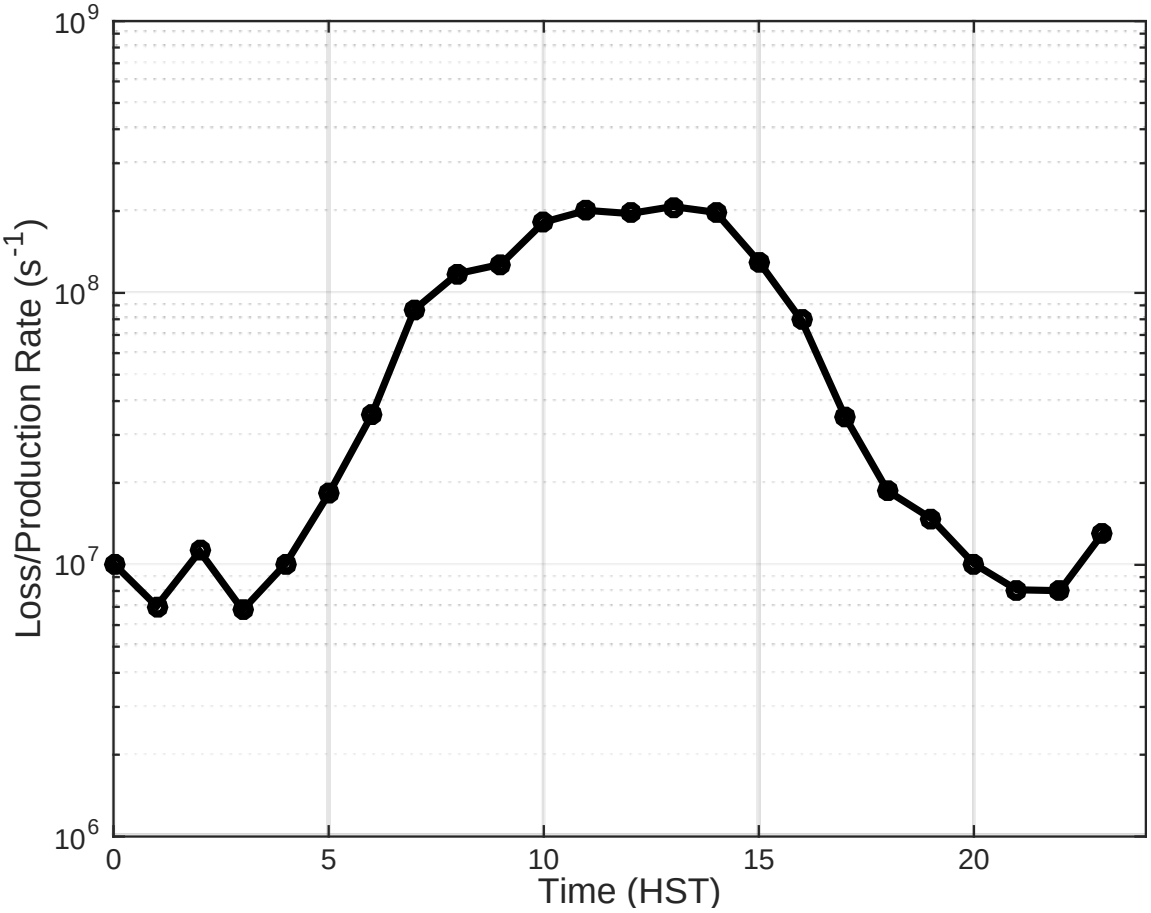

Figure 3: Estimated loss/production rate (s^{-1}) of OH calculated from INTEX-B CO, CH4, and OH data.

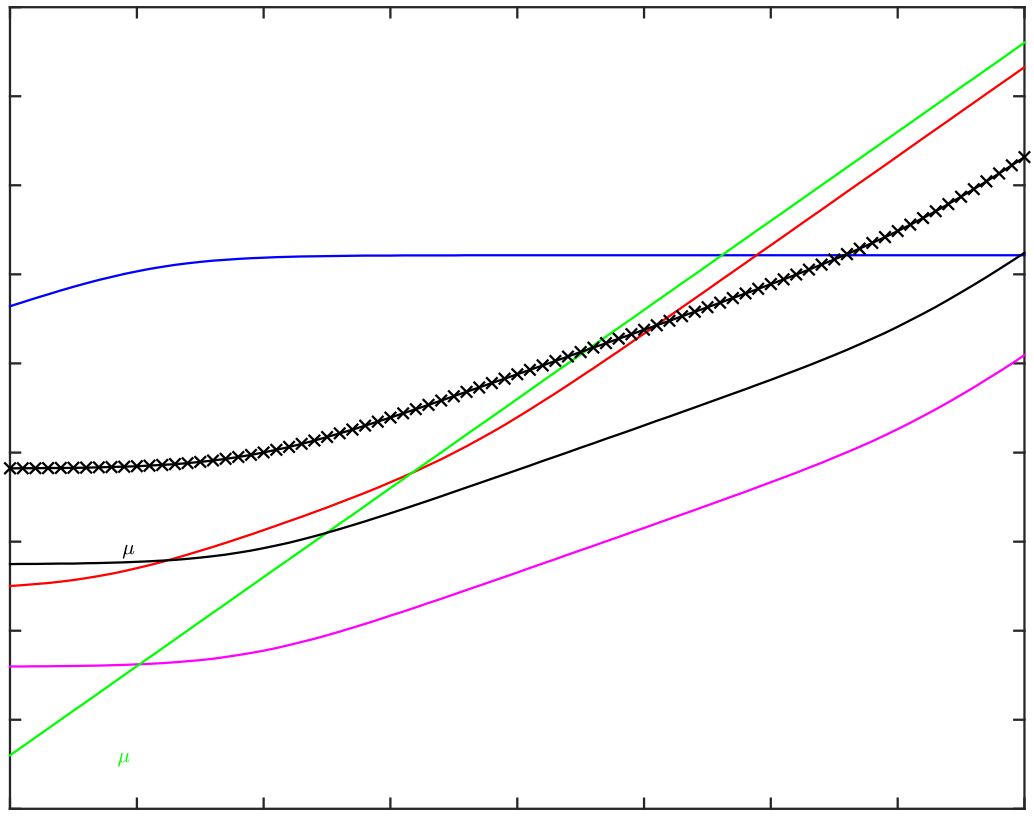

957

958 **Figure 4: Comparison of aqueous-phase oxidation paths near Kīlauea Volcano, Hawai'i. The rate of**

959 **conversion of S(IV) to S(VI) as a function of pH. Condition assumed are: [SO_2(g)] = 10 ppb; [NO_2(g)] =5**

960 **ppt; [H_2O_2 (g)]=1 ppb; [O_3(g)] = 20 ppb; [Fe(III)] = 1.0 µM; [Mn(II)]= 0.02 µM.**

Figure

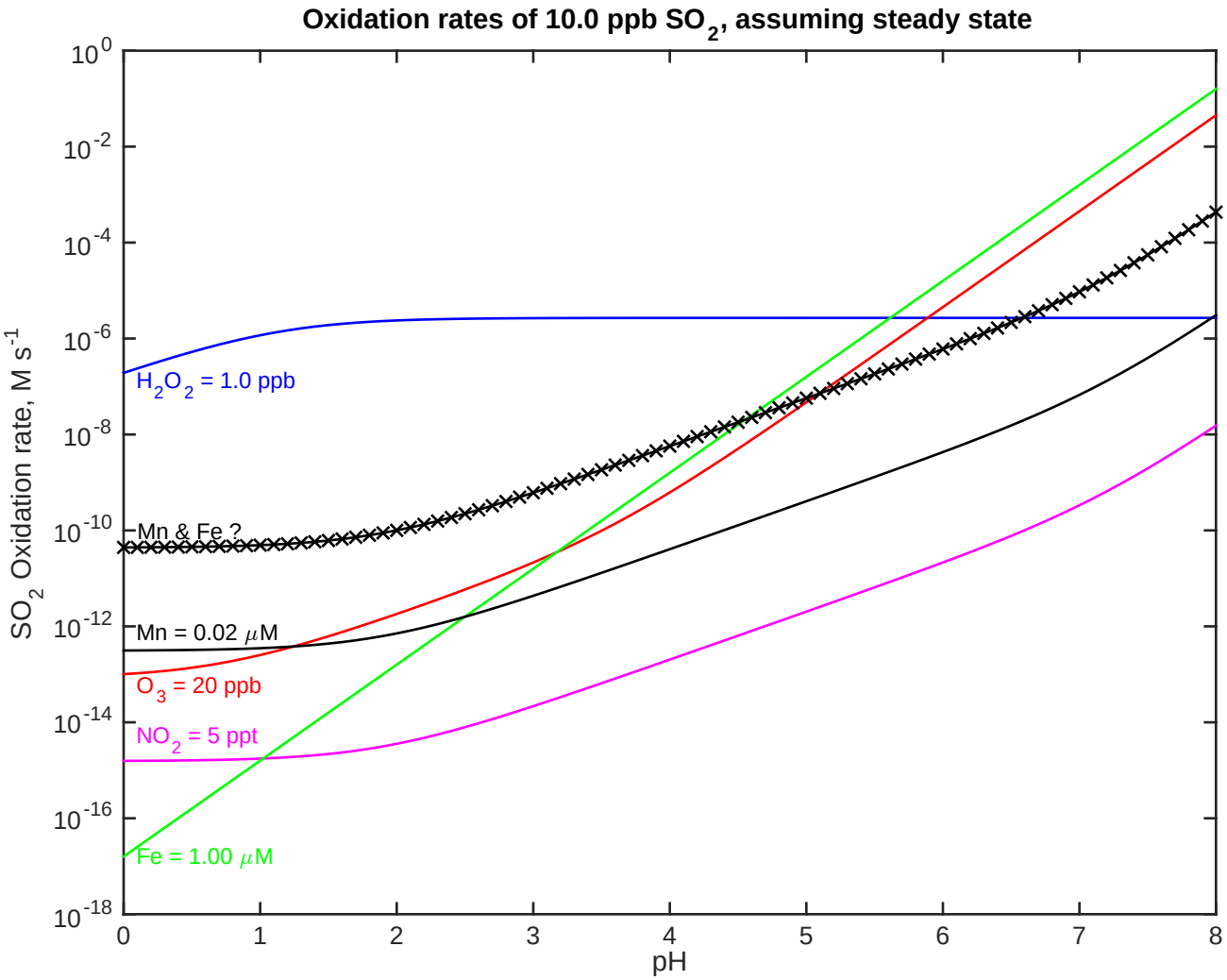
Oxidation rates of 10.0 ppb SO2, assuming steady state
SO2 Oxidation rate, M s-1
pH
H2O2 = 1.0 ppb
Mn & Fe ?
Mn = 0.02 μM
O3 = 20 ppb
NO2 = 5 ppt
Fe = 1.00 μM